



## RESEARCH LETTER

10.1002/2015GL065846

## Key Points:

- Atmospheric abundances of HCFC-133a and emissions have suddenly reversed in the last three years
- The sources of HCFC-133a to the atmosphere are likely from the production of HFC-134a
- In Europe, the emissions of HCFC-133a are less than 0.1 kt/yr while globally about 1.5 kt/yr

## Supporting Information:

- Text S1, Table S7, Figures S1–S8
- Table S1
- Table S2
- Table S3
- Table S4
- Table S5
- Table S6

## Correspondence to:

M. K. Vollmer,  
martin.vollmer@empa.ch

## Citation:

Vollmer, M. K., et al. (2015), Abrupt reversal in emissions and atmospheric abundance of HCFC-133a (CF<sub>3</sub>CH<sub>2</sub>Cl), *Geophys. Res. Lett.*, 42, 8702–8710, doi:10.1002/2015GL065846.

Received 20 AUG 2015

Accepted 20 SEP 2015

Accepted article online 6 OCT 2015

Published online 23 OCT 2015

## Abrupt reversal in emissions and atmospheric abundance of HCFC-133a (CF<sub>3</sub>CH<sub>2</sub>Cl)

Martin K. Vollmer<sup>1</sup>, Matt Rigby<sup>2</sup>, Johannes C. Laube<sup>3</sup>, Stephan Henne<sup>1</sup>, Tae Siek Rhee<sup>4</sup>, Lauren J. Gooch<sup>3</sup>, Angelina Wenger<sup>2</sup>, Dickon Young<sup>2</sup>, L. Paul Steele<sup>5</sup>, Ray L. Langenfelds<sup>5</sup>, Carl A. M. Brenninkmeijer<sup>6</sup>, Jia-Lin Wang<sup>7</sup>, Chang-Feng Ou-Yang<sup>8</sup>, Simon A. Wyss<sup>1</sup>, Matthias Hill<sup>1</sup>, David E. Oram<sup>3</sup>, Paul B. Krummel<sup>5</sup>, Fabian Schoenenberger<sup>1</sup>, Christoph Zellweger<sup>1</sup>, Paul J. Fraser<sup>5</sup>, William T. Sturges<sup>3</sup>, Simon O'Doherty<sup>2</sup>, and Stefan Reimann<sup>1</sup>

<sup>1</sup>Laboratory for Air Pollution and Environmental Technology, Empa, Swiss Federal Laboratories for Materials Science and Technology, Dübendorf, Switzerland, <sup>2</sup>School of Chemistry, University of Bristol, Bristol, UK, <sup>3</sup>Centre for Ocean and Atmospheric Sciences, School of Environmental Sciences, University of East Anglia, Norwich, UK, <sup>4</sup>Korea Polar Research Institute, KIOST, Incheon, South Korea, <sup>5</sup>CSIRO Oceans and Atmosphere, Aspendale, Victoria, Australia, <sup>6</sup>Air Chemistry Division, Max Planck Institute for Chemistry, Mainz, Germany, <sup>7</sup>Department of Chemistry, National Central University, Taiwan, <sup>8</sup>Department of Atmospheric Sciences, National Central University, Taiwan

**Abstract** Hydrochlorofluorocarbon HCFC-133a (CF<sub>3</sub>CH<sub>2</sub>Cl) is an anthropogenic compound whose consumption for emissive use is restricted under the Montreal Protocol. A recent study showed rapidly increasing atmospheric abundances and emissions. We report that, following this rise, the atmospheric abundance and emissions have declined sharply in the past three years. We find a Northern Hemisphere HCFC-133a increase from 0.13 ppt (dry-air mole fraction in parts per trillion) in 2000 to 0.50 ppt in 2012–mid-2013 followed by an abrupt drop to ~0.44 ppt by early 2015. Global emissions derived from these observations peaked at 3.1 kt in 2011, followed by a rapid decline of ~0.5 kt yr<sup>-2</sup> to reach 1.5 kt yr<sup>-1</sup> in 2014. Sporadic HCFC-133a pollution events are detected in Europe from our high-resolution HCFC-133a records at three European stations, and in Asia from samples collected in Taiwan. European emissions are estimated to be <0.1 kt yr<sup>-1</sup> although emission hot spots were identified in France.

### 1. Introduction

Hydrochlorofluorocarbons (HCFCs) can be viewed as the “second generation” ozone-depleting substances (ODSs). They have assisted the transition from the use of the first-generation ODSs, such as chlorofluorocarbons (CFCs) and halons, to chlorine- and bromine-free compounds, particularly in the industrial sectors of foam blowing, refrigeration, and as solvents [IPCC/TEAP, 2005]. The tropospheric lifetimes of the HCFCs and their potentials to destroy stratospheric ozone are considerably lower compared to those of the CFCs and halons. Nevertheless, many HCFCs also trap radiative heat efficiently and hence are potent greenhouse gases. Most ODSs are regulated internationally under the Montreal Protocol on Substances that Deplete the Ozone Layer, and its subsequent amendments. Today there is a global ban on the production and consumption for emissive use purposes of first-generation ODSs and there are transitional arrangements for the HCFCs, with a practical ban in industrialized countries and a phase out in developing countries.

HCFC-133a (CF<sub>3</sub>CH<sub>2</sub>Cl, 2-chloro-1,1,1-trifluoroethane, CAS 75-88-7) has only recently received attention, when its atmospheric history (1978 – 2012) was reconstructed based on the first measurements in archived air samples and those collected from aircraft at high altitudes [Laube et al., 2014]. HCFC-133a was found in stored air samples dating back to 1978 and both atmospheric abundances and derived global emissions from these observations revealed a rapid increase over the last three years (2010–2012) considered in that study.

Despite an estimated global emission of ~3 kt for the last year (2012) of the reported emissions [Laube et al., 2014], no purposeful end-product usage is known for this compound to date. Information on the usage of HCFC-133a is sparse. It is known as an intermediate product in the most direct method to synthesize the widely used refrigerant HFC-134a (1,1,1,2-tetrafluoroethane), in which trichloroethylene (CCl<sub>2</sub>=CHCl) is converted to HCFC-133a using hydrogen fluoride (HF) followed by replacement of the remaining chlorine through a reaction with excess HF and using metal catalysts in both steps [Rao, 1994; Banks and Sharratt, 1996; McCulloch and Lindley, 2003]. Some authors propose that any remaining HCFC-133a from this process is

recycled [Banks and Sharratt, 1996] or thermally oxidized [McCulloch and Lindley, 2003]. However, Banks and Sharratt [1996] estimated a release to the atmosphere of 5 g HCFC-133a per kilogram of produced HFC-134a for a factory in the United Kingdom in the mid-1990s. HCFC-133a is also known as an intermediate product in the syntheses of HFC-125 (1,1,1,2,2-pentafluoroethane) and HFC-143a (1,1,1-trifluoroethane) [Shanthan Rao *et al.*, 2015], and it is used for the production of pharmaceuticals, agrochemicals, and the anesthetic halothane [United Nations Environment Programme (UNEP)/Technology and Economic Assessment Panel (TEAP), 2014a] and potentially for the production of vinylidene fluoride [Shanthan Rao *et al.*, 2015]. While emissions during the production of HFCs appear to be an enticing explanation for recent atmospheric HCFC-133a levels, they could not explain its entire atmospheric history because HFCs were not mass produced before the mid-1990s, whereas HCFC-133a was found to be present in the atmosphere back to at least the late 1970s [Laube *et al.*, 2014].

Our knowledge on the atmospheric properties of HCFC-133a has increased in recent years. Its tropospheric sink is dominated by the reaction with the hydroxyl radical (OH) [Sander *et al.*, 2011, and references therein]. Recent laboratory and modeling studies by McGillen *et al.* [2015] revealed good agreement with these earlier studies and yielded a tropospheric lifetime of 4.65 years, which is also in good agreement with that proposed by Carpenter *et al.* [2014]. However, the recent study by McGillen *et al.* [2015], which included new measurements of UV photolysis rates, yielded a stratospheric lifetime of 103 years and is in disagreement with those reported by Laube *et al.* [2014] and Carpenter *et al.* [2014]. This difference is also the cause of the higher overall atmospheric lifetimes of 4.45 years reported by McGillen *et al.* [2015] compared to 4.0 years as proposed by Carpenter *et al.* [2014]. A radiative efficiency of  $0.15 \text{ W m}^{-2} \text{ ppb}^{-1}$  (with a 23% uncertainty based on a 5%–95% confidence interval) was recently computed for HCFC-133a based on measurements of its absorption cross section [Etminan *et al.*, 2014]. In the same study, the Global Warming Potential (GWP) for a 100 years time horizon was computed as 340, in reasonable agreement with the study by McGillen *et al.* [2015], in which a GWP of 380 was calculated.

## 2. Methods

### 2.1. In Situ and Flask Measurements

Our results are based on continuous (every 2 h) in situ measurements at four field stations, laboratory analyses of flask samples at Empa and at the University of East Anglia (UEA), and a previously published data set [Laube *et al.*, 2014] of HCFC-133a in samples of the Cape Grim Air Archive (CGAA) for the Southern Hemisphere collected at the Cape Grim Baseline Air Pollution Station, Tasmania [Langenfelds *et al.*, 1996, 2014]. In situ measurements were conducted at the remote baseline sites Jungfraujoch (3580 m above sea level (asl), Switzerland, 46.5°N, 8.0°E, since January 2013), Mace Head (Ireland, 53.3°N, 9.9°W, since May 2014), and Cape Grim (Tasmania, Australia, 40.7°S, 144.7°E, since July 2014). In addition, continuous in situ measurements were made at the suburban site Dubendorf (Switzerland, since December 2012). The in situ measurements were made with the “Medusa” gas chromatograph mass spectrometry (GCMS) technique [Miller *et al.*, 2008]. Analytes from 2 L of ambient air are collected on cold traps and separated on a CP-PoraBOND Q (0.32 mm ID × 25 m, 5 μm, Agilent Technologies) column in a GC (Agilent Technologies series 6890) followed by MS detection in selective ion mode (Agilent Technologies series 5975). The precision for the in situ air measurements is estimated at 1.5–2.0% ( $1\sigma$ ) for all four sites and is derived from the analysis of standards, samples of which are alternately analyzed with the air samples.

Flask samples were analyzed on the laboratory Medusa-GCMS at Empa. These included a set of archived air samples from various locations in the Northern Hemisphere dating back to 2000 (“Mini Air Archive North”) and a ship transect through the northern Pacific collected aboard the R/V *Araon* during the SHIPPO-2012 campaign [Park and Rhee, 2015; Vollmer *et al.*, 2015a]. Samples have also been collected at the South Korean Antarctic Station King Sejong (King George Island, South Shetland Islands, 62.2°S, 58.8°W) as part of a long-term network activity, with HCFC-133a analysis mainly for the 2012–2014 samples. We also analyzed a set of eight subsamples from the CGAA (2012–2014) to overlap and fill the gap between the CGAA record published by Laube *et al.* [2014] and the in situ measurements at Cape Grim and to enhance the data availability during the time of the reversal in the Southern Hemisphere.

The mean precision of the flask sample measurements at Empa was 1.2% ( $1\sigma$ ). Our results are reported on the Empa-2013 parts per trillion (ppt) level calibration scale for HCFC-133a, which was prepared as part of this study and with an estimated accuracy of 10%. The combined uncertainty of the Empa-based measurements was estimated from the calibration-scale uncertainty, the uncertainty of the standard propagation, and the

measurement precisions, totaling ~11% with the largest contribution from the calibration-scale uncertainty. Detailed information on the sampling, analysis, and the generation of a primary standard are given in the supporting information and by *Vollmer et al.* [2015a, 2015b].

Flask samples were also analyzed at the University of East Anglia (UEA). These included samples collected aboard regular aircraft flights within the project Civil Aircraft for the Regular Investigation of the atmosphere Based on an Instrument Container (CARIBIC) [*Brenninkmeijer et al.*, 2007]. Four flights between Frankfurt and South Africa between October 2009 and March 2010 as already published by *Laube et al.* [2014] are used. Four additional flights with previously unpublished HCFC-133a results from Frankfurt to Bangkok in 2013 (with samples between New Delhi and Bangkok) and one flight from Frankfurt to Cape Town in 2015 are also included. To complement our Northern Hemisphere record, we included two ground-based air samples collected in Greenland in 2008 as part of firn drilling activities.

The UEA analyses also included samples collected during two recent campaigns in Taiwan. In 2013, samples were collected from the Hengchun site (22.1°N, 120.7°E, 7 m asl), and in 2014 from Cape Fuguei (25.3°N, 121.5°E, 52 m asl). Air masses reached these sites predominantly from China and the Korean peninsula. Samples were collected into 3 L Silcosteel (Restek Corp.) treated stainless steel canisters using a diaphragm pump (Air Dimension Inc.). The samples were transferred to UEA and measured within 6 months of collection on two preconcentration GC systems, one coupled with a quadrupole MS (2013 and 2014 samples) [see *Leedham Elvidge et al.*, 2015] and the other one coupled with a high-sensitivity sector field MS (2014 samples only) [see *Laube et al.*, 2014]. Mean measurement precisions ( $1\sigma$ ) were 2.3% (quadrupole analysis) and 2.1% (sector analysis). Where samples were measured with both systems the results agreed within the uncertainty limits of the two instruments. If combined with the uncertainties of ~4% for the UEA calibration scale and its propagation, the overall accuracy is estimated at <8%.

To make the UEA and Empa measurements comparable, a calibration-scale conversion factor was determined by analysis of a suite of samples at both institutions (see supporting information). The conversion was found to be linear with an Empa/UEA conversion factor of 1.023. For this study all UEA results were multiplied by this factor to convert to the Empa-2013 calibration scale.

## 2.2. Global Chemical Transport Model and Inverse Methods

We employ an atmospheric box model combined with a Bayesian inverse method to derive global “top-down” emissions for HCFC-133a. For this we use the Advanced Global Atmospheric Gases Experiment (AGAGE) 12-box model [*Cunnold et al.*, 1983, 1997; *Rigby et al.*, 2013], which divides the atmosphere into four semi-hemispheres, separated at latitudes of 30°N and 30°S, and at the equator, and into three vertical layers separated at 500 hPa and 200 hPa. The horizontal separation is chosen such that all four semihemispheres in each respective layer contain a similar amount of air. We assumed a stratospheric lifetime of 103 years and a temperature-dependent reaction rate for OH as specified in *McGillen et al.* [2015], which led to an overall steady state lifetime in the model of 4.6 years.

To invert our observations for an emissions estimate, we use a Bayesian methodology in which an a priori estimate of the rates of change of the emissions is optimized using the observations [*Rigby et al.*, 2011, 2014]. The calculations are based on a simple a priori assumption that emissions grew by  $0 \pm 1 \text{ kt yr}^{-2}$  during the entire record. Emissions were estimated on an annual basis. However, to improve the seasonal agreement with the observations, we performed an ensemble of simulations in which the phase and amplitude of a sinusoidal emissions function were varied. We then optimized the emissions in the inversion assuming the seasonal variation function that provided the best fit to the observed seasonal cycle in the mole fractions. The derived emission seasonality is not reported below, as we propose that it is more likely to be due to seasonal errors in the box model transport parameters or loss rate than a real phenomenon. Since only annual emissions are presented, these potential seasonal errors are thought to have a negligible influence on our estimates. Uncertainties in the derived emissions include those due to the measurements and their model representation, along with potential biases such as errors in the assumed lifetime and the calibration scale [e.g., *Rigby et al.*, 2014].

With the exception of the data from the Taiwan campaigns, all of the surface flask observations were used in this global inversion, including the previously published CGAA record [*Laube et al.*, 2014]. We also used the in situ observations from the four stations. These were filtered to exclude potential pollution events [*Ruckstuhl et al.*, 2012] and binned into monthly background-air means. The inversion was provided with observations

on a monthly basis where all data in a respective box and for a respective month were averaged into one data point. CARIBIC results were not included in this inversion, mainly due to the inability to filter the data for background mole fractions, but they were used for model verification from comparison of reconstructed and observed mole fractions.

### 2.3. Inverse Methods for European Emissions

To derive European HCFC-133a source locations and emission estimates, we applied another Bayesian regional inversion system to the HCFC-133a observations (not filtered for pollution events) from Jungfraujoch (January 2013 to March 2015) and Mace Head (March 2014 to March 2015). This inversion system uses emission sensitivities as obtained from backward transport simulations with the Lagrangian particle dispersion model FLEXPART [Stohl *et al.*, 2005]. It follows the description by Stohl *et al.* [2009] and was previously applied to regional halocarbon emissions from Europe [Keller *et al.*, 2012] and China [Vollmer *et al.*, 2009]. Details of the transport simulations and the inversion settings are given in the supporting information. Lacking any reliable a priori information on the magnitude and spatial distribution of the HCFC-133a emissions, these were assumed to be homogeneously distributed over the continent and close to zero over the oceans. The total a priori emissions and their uncertainty for the inversion domain covering most of western and central Europe were set to  $0.02 \pm 0.06 \text{ kt yr}^{-1}$ ,  $0.05 \pm 0.15 \text{ kt yr}^{-1}$  and  $0.2 \pm 0.6 \text{ kt yr}^{-1}$  for a low-, base-, and high-sensitivity inversion, respectively. Furthermore, sensitivity inversions with decreased and increased a priori uncertainty, population-based a priori emission distribution, and different covariance designs were carried out to test the robustness of the results (see Table S7 in the supporting information). Deducing a temporal emission trend for the inversion domain is currently not possible given the relatively short record of continuous observations in Europe and the limited number of pollution events detected at these European sites.

## 3. Results

### 3.1. Observations

We present a Northern Hemisphere HCFC-133a record based on ground-based samples from 2000 to the present using flask sample and in situ measurements (in Figure 1). At northern midlatitudes HCFC-133a increased rapidly from 0.13 ppt (dry-air mole fraction in parts per trillion,  $10^{-12}$ ) in 2000 to a maximum of 0.55–0.57 ppt in 2012 to mid-2013, with a temporary halt in 2008, before abruptly declining to mole fractions of 0.49 ppt in early 2015. We confirm the Southern Hemisphere record published by Laube *et al.* [2014] for the overlapping period (2009–2012) and find a further increase in 2013 based on our Antarctic and Cape Grim measurements. It is followed by a plateau and a subsequent decline starting in mid-2014.

The Southern Hemisphere record reveals a clear seasonal cycle during the 2012–2014 period when observations are dense (see detail figure in supporting information). HCFC-133a seasonal extrema are in the austral summer and winter as expected based largely on the seasonality of the OH abundance, its major reactant for tropospheric removal. In contrast, the Northern Hemisphere seasonal cycle is unusual. While there is an indication from the 2012/2013 data of the expected HCFC-133a maximum in winter and minimum in summer, these extrema are considerably shifted during the subsequent year. For the in situ measurements of all four Northern Hemisphere stations the minima are shifted by about 4 months to the end of the year. This is likely a first-order result of the rapidly declining emissions (see below) combined with a seasonality in the abundance of the OH radical. Our Northern Hemisphere observations for 2006–2009 are consistent with the early intermittent Southern Hemisphere maximum found for 2007 by Laube *et al.* [2014]. However, the most recent and significantly larger reversal of the HCFC-133a trend in both hemispheres could not be detected from the observations reported by Laube *et al.* [2014] because of the lack of recent Northern Hemisphere samples, which now show (this work) a stagnant abundance by 2012 and because the Southern Hemisphere measurements stopped shortly before the onset of a significant slowdown in this hemisphere. The results of the SHIPPO-2012 North Pacific expeditions feature a significant range of mole fractions. This is caused by the large latitude range of the air mass origins in a latitude band where strong mole fraction gradients are expected due to latitudinally varying emissions. A similar variability for these samples was found in other compounds [Vollmer *et al.*, 2015a].

Our derived emissions (see below) are used to run the 12-box model in a forward mode in order to simulate the observations. In general, the model reproduces the observed mole fractions within the combined uncertainties. The modeled mole fractions shown in Figure 1 are for the model surface boxes 30°N to 90°N (in red) and 30°S to 90°S (in black). For the mean Northern Hemisphere we find HCFC-133a increased from 0.13 ppt in 2000 to 0.50 ppt in 2012 to mid-2013 followed by a decline to 0.44 ppt by early 2015.

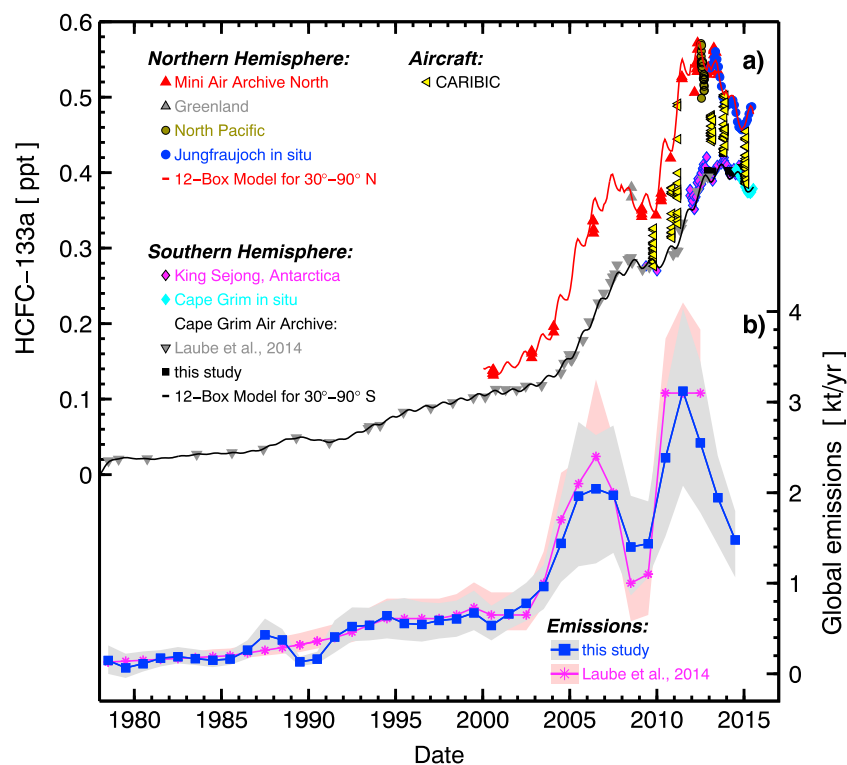


**Figure 1.** Atmospheric records (a) and emissions (b) of HCFC-133a ( $\text{CF}_3\text{CH}_2\text{Cl}$ ). Abundances are reported as dry-air mole fractions in parts per trillion (ppt) for flask samples collected: in the Northern Hemisphere at various locations during clean air conditions, from the North Pacific during the SHIPPO-2012 expedition and from Greenland surface air in firn; in the Southern Hemisphere from the Korean Antarctic Station King Sejong and at Cape Grim (Tasmania); at high altitude as part of the project CARIBIC from aircraft sampling in both hemispheres. Monthly means of background-filtered measurements from in situ measurements at Jungfraujoch (Switzerland) and Cape Grim (Tasmania) are also shown, those from Dubendorf (Switzerland) and Mace Head (Ireland) are not shown here. The solid lines are modeled mole fractions for the model surface boxes  $30^\circ\text{N}$  to  $90^\circ\text{N}$  (in red) and  $30^\circ\text{S}$  to  $90^\circ\text{S}$  (in black). Model-derived emissions from this study are shown as solid blue lines with 16/84 percentile shading and are compared to those derived by Laube *et al.* [2014]. See supporting information for a detailed view of the most recent years.

The apparent mismatch between modeled and observed abundances in the Northern Hemisphere during the steep increase in the 2010s is likely caused by the large latitudinal gradient—the mole fractions of the surface box  $0^\circ$  to  $30^\circ\text{N}$  (not shown in Figure 1, see supporting information) are considerably lower compared to those plotted in Figure 1. However, for the Southern Hemisphere the model slightly underestimates the observations presented here (mid to high latitude) despite virtually no latitudinal gradient in the Southern Hemisphere (Figure S1).

The CARIBIC samples for the flights used here are generally from altitudes higher than 10 km. Because of this large distance from ground and the general absence of areas with strong uplift of ground-based air masses we conclude that the influence of regional ground pollution is small and that the measured mole fractions represent mostly background conditions for these altitudes. The mole fractions from these samples are generally bracketed by the modeled mole fractions in the two high-latitude model boxes. However, the highest mole fractions of the flights in late 2013 slightly exceed the monthly mean values at the in situ stations (Figures 1 and S1). This can have been partly caused by a lag of the declining trend due to the transit time of surface air masses to these altitudes ( $>11$  km) or by input from fresh pollution, which was also found for some other compounds in some of these samples [Kloss *et al.*, 2014].

Our results from the in situ measurements at four stations and from the two sampling campaigns in Taiwan are shown in Figure 2. All three Northern Hemisphere stations reveal the same trend of declining abundances and the same seasonal background variability. They also exhibit occasional pollution events with magnitudes in the mole fraction typically reaching 2 to 3 times the mole fractions of the background signal. When comparing the Dubendorf and Jungfraujoch records we find similar magnitudes of pollution events and only slightly

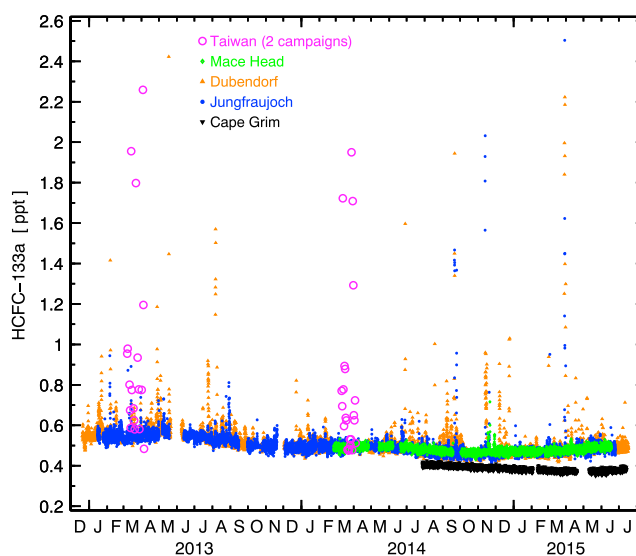


**Figure 2.** Atmospheric abundances of HCFC-133a ( $\text{CF}_3\text{CH}_2\text{Cl}$ ) from in situ measurements at Jungfraujoch (Switzerland), Mace Head (Ireland), Cape Grim (Tasmania, Australia), and suburban Dubendorf (Switzerland) and from flask samples collected during two campaigns at Hengchun and Cape Fuguei (Taiwan). The abundances are given as dry-air mole fractions in parts per trillion (ppt) on the Empa-2013 calibration scale. The three European stations exhibit similar background records. Pollution events can also be observed, mainly at Dubendorf and Jungfraujoch and to a lesser extent at Mace Head. Similarly, elevated HCFC-133a is found in some of the Taiwan samples. One or two sample results each with the highest mole fraction are not shown for each of Jungfraujoch, Dubendorf, and Taiwan. There are no pollution events detected at the background station Cape Grim despite occasional air mass advection from the densely populated Melbourne area which, for example, exhibit significantly polluted HFC-134a levels.

larger frequency of events occurring at Dubendorf. These pollution events are much less frequent than those found for most other compounds measured at the two sites [Vollmer *et al.*, 2015b; O'Doherty *et al.*, 2014; Vollmer *et al.*, 2011] and are suggestive of fewer and more remote sources. The  $\sim 1.5$  year record at Mace Head exhibits only two pollution events (in November 2014), whereas pollution events are absent at Cape Grim despite occasional interception of air masses from populated areas at both sites which, for example, show significantly polluted HFC-134a levels. The flask measurements from Taiwan exhibit similarly elevated mole fractions in “polluted” air as Jungfraujoch and Dubendorf. We suspect that these are caused by HCFC-133a emissions from China and the Korean Peninsula, which are the major air mass advection directions to the Taiwan sampling sites. Air trajectory analysis and complementary measurements of local wind speed have indicated no significant elevations of HCFC-133a mole fractions associated with air masses sensitive to emissions from Taiwan.

### 3.2. Emissions

Our derived global top-down emission estimates are shown in Figure 1. For the earlier part of the record the emissions were increasing from  $\sim 0.2 \text{ kt yr}^{-1}$  in the late 1970s to a first maximum in 2006 ( $2.0 \text{ kt yr}^{-1}$ ). This was followed by a decline to  $\sim 1.4 \text{ kt yr}^{-1}$  in 2008/2009 and a subsequent rapid increase after that. Our emissions agree within the combined uncertainties with those derived by Laube *et al.* [2014] for the overlapping period. The focus of this study, however, is on the emissions of the five most recent years. We find that these emissions have peaked sharply at  $3.1 \text{ kt yr}^{-1}$  in 2011 and declined rapidly since then at  $\sim 0.5 \text{ kt yr}^{-2}$  to  $1.5 \text{ kt yr}^{-1}$  in 2014. This is equivalent to a reduction of  $>50\%$  in 3 years.

Our results for the European emission estimates are shown in Figure 3. Given the observed time series with relatively few pollution events, we expected that the major emissions are from a few isolated locations and that they may also vary strongly in time. Both pose major challenges to the applied Bayesian inversion, which assumes constant emissions in time and is usually guided toward a meaningful solution by the use of best available a priori emission estimates. Hence, the obtained results can only give a first impression of possible source locations and strengths. Nevertheless, it is encouraging that despite these limitations the inversion obtained a posteriori emissions that indicate two emission hot spots in France, where emissions are well constrained by the observations. Elsewhere, emissions were mainly reduced. The simulated time series at the two

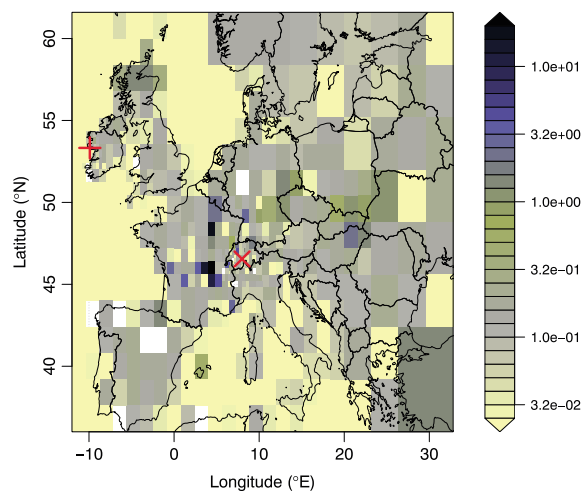


**Figure 3.** Posterior HCFC-133a emission distribution ( $\mu\text{g km}^{-2} \text{s}^{-1}$ ) in Europe obtained for the base inversion. In situ observations from Jungfrauoch (Switzerland, January 2013 to March 2015, red cross) and Mace Head (Ireland, March 2014 to March 2015, red plus) are used in this inversion. White areas indicate grid cells with zero emissions. Regions of emissions were identified in France (regions Lyon and  $\sim 150$  km east of Paris).

observational sites were generally improved using a posteriori emissions (see supporting information for a more detailed discussion of the inversion results and Table S7 for comparison statistics). The largest emissions were obtained for the grid cells covering the region of Lyon followed by a smaller hot spot  $\sim 150$  km east of Paris. These locations proved to be relatively insensitive to the choice of the inversion settings and were similar for all sensitivity inversions. Total a posteriori domain emissions ranged from  $56 \pm 10 \text{ t yr}^{-1}$  to  $96 \pm 10 \text{ t yr}^{-1}$  for the different sensitivity inversions (Table S7) at least 1 order of magnitude smaller compared to the global emissions. The French a posteriori emissions, including the two hot spots, were very similar in all sensitivity inversions ( $13\text{--}18 \pm 2 \text{ t yr}^{-1}$ ) and contributed between one sixth and one third of the domain total. This fraction may be an underestimation because the chosen homogeneous a priori emission distribution used large emissions also in relatively sparsely populated and remote regions that could not be adjusted adequately by the inversion.

### 3.3. Discussion

Given their rapid decline, we conclude that the large reduction in global emissions is related to the prevention of emissions from activities, which are/were under immediate and direct human control. A rapid reduction like the one we derive would not be possible for more diffusive sources such as widespread “banks” of stored chemicals in equipment or products (e.g., foams, refrigeration units, and fire extinguishing units). However, direct end-user applications are also absent to the best of our knowledge, partially because of the compound’s toxicity [ECETOC, 1990] and its ban by the Montreal Protocol. We speculate that large emissions reductions have been made in factories where HCFC-133a occurs as an intermediate in the synthesis of other chemicals or as a by-product, both with direct release (rather than an impurity in the end-product).

The most likely explanation to us for the derived HCFC-133a emissions decline is a reduction in its release during the production processes of HFC-134a and HFC-125 [Shanthan Rao *et al.*, 2015]. The synthesis of both these HFCs is typically performed in a two-step reaction. In the case of HFC-134a, trichloroethylene is converted to HCFC-133a by catalytic vapor phase fluorination using hydrogen fluoride, and then further fluorinated to HFC-134a [Shanthan Rao *et al.*, 2015]. It appears that any unreacted HCFC-133a can be recycled into the second production step; however, it is unclear if this is a commonly used practice. In the case of HFC-125, perchloroethylene is hydrofluorinated to HFC-125 with several intermediate/by-products, one of which is HCFC-133a, for which it is stated in one of the relevant patents that it is not economical to recycle [Shields and Ewing, 1999]. Because of its toxicity and carcinogenicity, the two individual steps of the reactions are probably geographically collocated and a transport (and hence potential leakage) of large amounts of pure HCFC-133a is unlikely (M. Nappa, personal communication, 2015). In contrast to declining emissions of HCFC-133a, the consumption and hence the production of these HFCs has grown rapidly over the past years [United Nations Environment Programme (UNEP)/Technology and Economic Assessment Panel (TEAP), 2014b;

Zhang and Wang, 2014; G. Velders, personal communication, 2015, data through 2011]. Unless production methods have significantly shifted, this apparent contrast supports the hypothesis of the HCFC-133a emissions decline due to better containment (including better catalytic conversion techniques) of HCFC-133a in these production plants rather than a reduced overall HFC production. Furthermore, based on our global results, it is very unlikely that HCFC-133a occurs as an impurity in the HFC end products because such diffusive emissions could not be reduced at the high rates we derived. This is supported by our regional emission map for Europe where we find emissions from hot spots rather than widespread diffusive sources. Also, for our Dubendorf results we find large HFC pollution events without concordant HCFC-133a pollution, whereas at Jungfraujoch, the HCFC-133a pollution events were accompanied by relatively minor HFC pollution. In addition, we find undetectable HCFC-133a in a diluted HFC-134a sample corresponding to  $< 10^{-4}\%$  (molar) of HCFC-133a in high-purity HFC-134a. These observations are partially supportive but not a general proof of the absence of HCFC-133a impurities in HFCs because the HFCs emitted within the footprints of the Dubendorf site are not globally representative for all commercial HFC sources.

Historical HCFC-133a emissions cannot be entirely attributed to HFC production because HCFC-133a was present in the atmosphere long before HFC production started [Laube *et al.*, 2014]. Nevertheless, HCFC-133a emissions were comparably small until 2003 when they started to increase rapidly. It is possible that earlier HCFC-133a emissions were related to halothane production and that this source has become insignificant due to the phase out of this anesthetic [Vollmer *et al.*, 2015a]. The pronounced earlier HCFC-133a reversal in atmospheric abundance and emissions in 2009/2010 is likely related to changes in HFC production alone with a potential change in production procedures [Laube *et al.*, 2014] or a shutdown of smaller and potentially more polluting HFC plants during reduced activities at times of the global financial crisis. Further research is needed to understand whether halothane and HFC production alone could explain the historic HCFC-133a emissions, or if some of the other potential sources, e.g., from the production of pharmaceuticals and agrochemicals (see section 1) may significantly contribute to HCFC-133a emissions.

Strikingly similar global abundance and emission reversal patterns were recently found for HCFC-31 ( $\text{CH}_2\text{ClF}$ ) [Schoenenberger *et al.*, 2015]. The emissions of this compound, which were estimated based on the first atmospheric observations, have peaked in 2011, at a similar time as those of HCFC-133a, and have been declining rapidly after that, presumably due to better containment of this compound during the production of HFC-32 ( $\text{CH}_2\text{F}_2$ ), where HCFC-31 occurs as an intermediate product [Schoenenberger *et al.*, 2015].

#### 4. Conclusion

Based on a wealth of atmospheric observations, we derive a rapid recent decline in global HCFC-133a emissions. While our results suggest direct and immediate human control on these reductions, the mechanisms, which have led to this reduction, remain to a large extent speculative. Furthermore, the incentives and driving mechanism that have triggered these activities remain also unknown—foremost it is unclear if they were deliberate or as an unintended consequence of other activities. One possible explanation is that regulations or economic incentives have led to the observed reduction in emissions. We hypothesize that HCFC-133a emissions are emitted at the production-facility level. From the ongoing decline, we conclude that the reduction was not a one-step measure (otherwise the emissions would have stopped decreasing). In contrast, the rate at which our modeled emissions decline ( $\sim 0.5 \text{ kt yr}^{-2}$ ) has only marginally decreased over the past 4 years and is suggestive of continuously evolving containment activities. However, the most recent months of observations are suggestive of a slowdown in the atmospheric decline in HCFC-133a mole fractions which could point to a stabilization of the global emissions in the near future.

#### Acknowledgments

We thank the station personnel at Jungfraujoch (the Fischer and Oetz families), Mace Head (Gerard Spain), and Cape Grim (particularly Jeremy Ward and Nigel Somerville) for their continuous logistical support for the Medusa-GCMS operations; the many contributors involved in providing flask samples, in particular, the staff of the National Central University (Taiwan), and the CARIBIC team; Mack McFarland and Mario Nappa (DuPont)

#### References

- Banks, R. E., and P. N. Sharratt (1996), Environmental impacts of the manufacture of HFC-134a, *Tech. Rep.*, Department of Chemistry and Department of Chemical Engineering, UMIST, Manchester.
- Breninkmeijer, C. A. M., et al. (2007), Civil Aircraft for the regular investigation of the atmosphere based on an instrumented container: The new CARIBIC system, *Atmos. Chem. Phys.*, 7(18), 4953–4976, doi:10.5194/acp-7-4953-2007.
- Carpenter, L. J., et al. (2014), Ozone-depleting substances (ODSs) and other gases of interest to the Montreal Protocol, in *Scientific Assessment of Ozone Depletion: 2014, Global Ozone Research and Monitoring Project—Rep. 55*, chap. 1, World Meteorol. Organ., Geneva, Switzerland.
- Cunnold, D. M., R. G. Prinn, R. A. Rasmussen, P. G. Simmonds, F. N. Alyea, C. A. Cardelino, A. J. Crawford, P. J. Fraser, and R. D. Rosen (1983), The atmospheric lifetime experiment 3. Lifetime methodology and application to 3 years of  $\text{CFCl}_3$  data, *J. Geophys. Res.*, 88(C13), 8379–8400.
- Cunnold, D. M., R. F. Weiss, R. G. Prinn, D. Hartley, P. G. Simmonds, P. J. Fraser, B. Miller, F. N. Alyea, and L. Porter (1997), GAGE/AGAGE measurements indicating reductions in global emissions of  $\text{CCl}_3\text{F}$  and  $\text{CCl}_2\text{F}_2$  in 1992–1994, *J. Geophys. Res.*, 102(D1), 1259–1269.



for clarifications on HFC production; Guus Velders (National Institute for Public Health and the Environment, RIVM) for providing unpublished HFC consumption data; and the AGAGE team for continuous technical and scientific support. This project is conducted under the auspices of the European FP7 Infrastructure Project "Integrated Non-CO<sub>2</sub> Greenhouse gas Observing System" (InGOS), and the European Metrology Research Programme ENV52 project "Metrology for high-impact greenhouse gases, HIGHGAS." Funding is also provided for the measurements at Jungfraujoch by the Swiss Federal Office for the Environment (FOEN) within the project HALCLIM; and by the International Foundation High Altitude Research Stations Jungfraujoch and Gornergrat (HFSJG). Operation of in situ measurements at the Mace Head research station is supported by the Department of Energy and Climate Change (DECC, UK); contract GA0201 to the University of Bristol. The Cape Grim research station is funded and managed by the Australian Bureau of Meteorology with the science program jointly managed and funded by CSIRO and the Bureau of Meteorology. Support for the Antarctic work comes from the Swiss State Secretariat for Education and Research and Innovation (SERI) and the National Research Foundation of Korea for the Korean-Swiss Science and Technology Cooperation Program. The UEA measurements were funded by UK NERC (grant NE/J016012) and the National Centre for Atmospheric Science (NCAS). The Taiwan Ministry of Science and Technology supported the work in Taiwan. M.R. and J.C.L. are supported by Advanced Research Fellowships from the UK Natural Environment Research Council (NERC) (NE/1021365/1 and NE/1021918/1, respectively). T.S.R. is supported by the Korean Polar Research Programs PE13410 and PP15101. UEA work was also supported by Award NERC IOF award NE/J016012/1 and a NERC Studentship to L.G. Data used in this study are available from the supporting information and the corresponding author.

The Editor thanks four anonymous reviewers for their assistance in evaluating this paper.

- ECETOC (1990), 1-Chloro-2,2,2-trifluoroethane (HFA-133a) CAS:75-88-7, *Tech. Rep.*, JACC 014, European Chemical Industry Ecology and Toxicology Centre, Brussels.
- Etminan, M., E. J. Highwood, J. C. Laube, R. McPheat, G. Marston, K. P. Shine, and K. M. Smith (2014), Infrared absorption spectra, radiative efficiencies, and global warming potentials of newly-detected halogenated compounds: CFC-113a, CFC-112 and HCFC-133a, *Atmosphere*, *5*, 473–483, doi:10.3390/atmos5030473.
- IPCC/TEAP (2005), *Special Report on Safeguarding the Ozone Layer and the Global Climate System: Issues Related to Hydrofluorocarbons and Perfluorocarbons. Prepared by Working Group I and III of the Intergovernmental Panel on Climate Change, and the Technology and Economic Assessment Panel*, 488 pp., Cambridge Univ. Press, Cambridge, U. K., and New York.
- Keller, C. A., et al. (2012), European emissions of halogenated greenhouse gases inferred from atmospheric measurements, *Environ. Sci. Technol.*, *46*, 217–225, doi:10.1021/es202453j.
- Kloss, C., M. J. Newland, D. E. Oram, P. J. Fraser, C. A. M. Brenninkmeijer, T. Röckmann, and J. C. Laube (2014), Atmospheric abundances, trends and emissions of CFC-216ba, CFC-216ca and HCFC-225ca, *Atmosphere*, *5*, 420–434, doi:10.3390/atmos5020420.
- Langenfelds, R. L., P. J. Fraser, R. J. Francey, L. P. Steele, L. W. Porter, and C. E. Allison (1996), The Cape Grim air archive: The first seventeen years, 1978–1995, in *Baseline Atmospheric Program (Australia) 1994–95*, edited by R. J. Francey, A. L. Dick, and N. Derek, pp. 53–70, Bureau of Meteorology and CSIRO Division of Atmospheric Research, Australian Bureau of Meteorology and CSIRO Marine and Atmospheric Research, Melbourne, Australia.
- Langenfelds, R. L., P. B. Krummel, P. J. Fraser, L. P. Steele, J. Ward, and N. T. Somerville (2014), Archiving of Cape Grim air, in *Baseline Atmospheric Program Australia 2009–2010*, edited by N. Derek, P. B. Krummel, and S. J. Cleland, pp. 44–45, Australian Bureau of Meteorology and CSIRO Marine and Atmospheric Research, Melbourne, Australia.
- Laube, J. C., et al. (2014), Newly detected ozone-depleting substances in the atmosphere, *Nat. Geosci.*, *7*, 266–269, doi:10.1038/NCEO2109.
- Leedham Elvidge, E. C., D. E. Oram, J. C. Laube, A. K. Baker, S. A. Montzka, S. Humphrey, D. A. O'Sullivan, and C. A. M. Brenninkmeijer (2015), Increasing concentrations of dichloromethane, CH<sub>2</sub>Cl<sub>2</sub>, inferred from CARIBIC air samples collected 1998–2012, *Atmos. Chem. Phys.*, *15*(4), 1939–1958, doi:10.5194/acp-15-1939-2015.
- McCulloch, A., and A. A. Lindley (2003), From mine to refrigeration: A life cycle inventory analysis of the production of HFC-134a, *Int. J. Refrig.*, *26*, 865–872.
- McGillen, M. R., F. Bernard, E. L. Fleming, and J. B. Burkholder (2015), HCFC-133a (CF<sub>3</sub>CH<sub>2</sub>Cl): OH rate coefficient, UV and infrared absorption spectra, and atmospheric implications, *Geophys. Res. Lett.*, *42*, 6098–6105, doi:10.1002/2015GL064939.
- Miller, B. R., R. F. Weiss, P. K. Salameh, T. Tanhua, B. R. Grealley, J. Mühle, and P. G. Simmonds (2008), Medusa: A sample preconcentration and GC/MS detector system for in situ measurements of atmospheric trace halocarbons, hydrocarbons, and sulfur compounds, *Anal. Chem.*, *80*(5), 1536–1545, doi:10.1021/ac702084k.
- O'Doherty, S., et al. (2014), Global emissions of HFC-143a (CH<sub>3</sub>CF<sub>3</sub>) and HFC-32 (CH<sub>2</sub>F<sub>2</sub>) from in situ and air archive atmospheric observations, *Atmos. Chem. Phys.*, *14*, 9249–9258, doi:10.5194/acp-14-9249-2014.
- Park, K., and T. S. Rhee (2015), Source characterization of carbon monoxide and ozone over the Northwestern Pacific in summer 2012, *Atmos. Environ.*, *111*, 151–160, doi:10.1016/j.atmosenv.2015.04.015.
- Rao, V. N. M. (1994), Alternatives to chlorofluorocarbons (CFCs), in *Organofluorine Chemistry: Principles and Commercial Applications*, edited by R. E. Banks, B. E. Smart, and J. C. Tatlow, pp. 159–175, Topics in Applied Chemistry, Plenum Press, New York.
- Rigby, M., A. L. Ganesan, and R. G. Prinn (2011), Deriving emissions from sparse mole-fraction time series, *J. Geophys. Res.*, *116*, D08306, doi:10.1029/2010JD015401.
- Rigby, M., et al. (2013), Re-evaluation of lifetimes of the major CFCs and CH<sub>3</sub>CCl<sub>3</sub> using atmospheric trends, *Atmos. Chem. Phys.*, *13*, 2691–2702, doi:10.5194/acp-13-2691-2013.
- Rigby, M., et al. (2014), Recent and future trends in synthetic greenhouse gas radiative forcing, *Geophys. Res. Lett.*, *41*, 2623–2630, doi:10.1002/2013GL059099.
- Ruckstuhl, A. F., S. Henne, S. Reimann, M. Steinbacher, M. K. Vollmer, S. O'Doherty, B. Buchmann, and C. Hueglin (2012), Robust extraction of baseline signal of atmospheric trace species using local regression, *Atmos. Meas. Tech.*, *5*, 2613–2624, doi:10.5194/amt-5-2613-2012.
- Sander, S. P., et al. (2011), Chemical kinetics and photochemical data for use in atmospheric studies, evaluation no. 17 of the NASA panel for data evaluation, JPL Publ., 10-6, Jet Propul. Lab., Pasadena.
- Schoenenberger, F., M. K. Vollmer, M. Rigby, M. Hill, P. J. Fraser, P. B. Krummel, R. L. Langenfelds, T. S. Rhee, T. Peter, and S. Reimann (2015), First observations, trends and emissions of HCFC-31 (CH<sub>2</sub>ClF) in the global atmosphere, *Geophys. Res. Lett.*, *42*, 7817–7824, doi:10.1002/2015GL064709.
- Shanthan Rao, P., B. Narsaiah, Y. Rambabu, M. Sridhar, and K. V. Raghavan (2015), Catalytic processes for fluorochemicals: Sustainable alternatives, in *Industrial Catalysis and Separations: Innovations for Process Intensification*, edited by K. V. Raghavan and B. M. Reddy, pp. 407–435, Apple Academic Press, Toronto.
- Shields, C., and P. Ewing (1999), Process for the manufacture of pentafluoroethane, US Patent 5,962, 753.
- Stohl, A., C. Forster, A. Frank, P. Seibert, and G. Wotawa (2005), Technical note: The Lagrangian particle dispersion model FLEXPART version 6.2, *Atmos. Chem. Phys.*, *5*, 2461–2474, doi:10.5194/acp-5-2461-2005.
- Stohl, A., et al. (2009), An analytical inversion method for determining regional and global emissions of greenhouse gases: Sensitivity studies and application to halocarbons, *Atmos. Chem. Phys.*, *9*, 1597–1620, doi:10.5194/acp-9-1597-2009.
- United Nations Environment Programme (UNEP)/Technology and Economic Assessment Panel (TEAP) (2014a), May 2014 TEAP report, in *TEAP 2014 Progress Report*, vol. 1, pp. 47, United Nations Environment Programme, Nairobi, Kenya.
- United Nations Environment Programme (UNEP)/Technology and Economic Assessment Panel (TEAP) (2014b), May 2014 TEAP report, in *Decision XXV/5 Task Force Report: Additional Information to Alternatives on ODS (Final Report)*, vol. 4, pp. 141, United Nations Environment Programme, Nairobi, Kenya.
- Vollmer, M. K., et al. (2009), Emissions of ozone-depleting halocarbons from China, *Geophys. Res. Lett.*, *36*, L15823, doi:10.1029/2009GL038659.
- Vollmer, M. K., et al. (2011), Atmospheric histories and global emissions of the anthropogenic hydrofluorocarbons HFC-365mfc, HFC-245fa, HFC-227ea, and HFC-236fa, *J. Geophys. Res.*, *116*, D08304, doi:10.1029/2010JD015309.
- Vollmer, M. K., T. S. Rhee, M. Rigby, D. Hofstetter, M. Hill, F. Schoenenberger, and S. Reimann (2015a), Modern inhalation anesthetics: Potent greenhouse gases in the global atmosphere, *Geophys. Res. Lett.*, *42*, 1606–1611, doi:10.1002/2014GL062785.
- Vollmer, M. K., S. Reimann, M. Hill, and D. Brunner (2015b), First observations of the fourth generation synthetic halocarbons HFC-1234yf, HFC-1234ze(E), and HCFC-1233zd(E) in the atmosphere, *Environ. Sci. Technol.*, *49*, 2703–2708, doi:10.1021/es505123x.
- Zhang, J., and C. Wang (2014), China's hydrofluorocarbon challenge, *Nature*, *4(11)*, 943–945.